

Research outputs 2014 to 2021

---

11-1-2021

## Influence of pressure, temperature and organic surface concentration on hydrogen wettability of caprock, implications for hydrogen geo-storage

Muhammad Ali

Nurudeen Yekeen

Nilanjan Pal

Alireza Keshavarz

*Edith Cowan University*

Stefan Iglauer

*Edith Cowan University*

*See next page for additional authors*

Follow this and additional works at: <https://ro.ecu.edu.au/ecuworkspost2013>

 Part of the [Engineering Commons](#)

---

[10.1016/j.egyr.2021.09.016](https://doi.org/10.1016/j.egyr.2021.09.016)

Ali, M., Yekeen, N., Pal, N., Keshavarz, A., Iglauer, S., & Hoteit, H. (2021). Influence of pressure, temperature and organic surface concentration on hydrogen wettability of caprock; implications for hydrogen geo-storage. *Energy Reports*, 7, 5988-5996.

<https://doi.org/10.1016/j.egyr.2021.09.016>

This Journal Article is posted at Research Online.

<https://ro.ecu.edu.au/ecuworkspost2013/11745>

---

**Authors**

Muhammad Ali, Nurudeen Yekeen, Nilanjan Pal, Alireza Keshavarz, Stefan Iglauer, and Hussein Hoteit



## Research paper

# Influence of pressure, temperature and organic surface concentration on hydrogen wettability of caprock; implications for hydrogen geo-storage



Muhammad Ali <sup>a,b,\*</sup>, Nurudeen Yekeen <sup>c</sup>, Nilanjan Pal <sup>a</sup>, Alireza Keshavarz <sup>d</sup>, Stefan Iglauer <sup>d</sup>, Hussein Hoteit <sup>a,\*\*</sup>

<sup>a</sup> Physical Science and Engineering Division, King Abdullah University of Science and Technology (KAUST), Thuwal, 23955, Saudi Arabia

<sup>b</sup> Western Australia School of Mines, Minerals, Energy and Chemical Engineering, Curtin University, Kensington 6151, Western Australia, Australia

<sup>c</sup> Department of Chemical & Petroleum Engineering, Faculty of Engineering, Technology and Built Environment, UCSI University, 56000, Kuala Lumpur, Malaysia

<sup>d</sup> School of Engineering, Edith Cowan University, Joondalup 6027, WA, Australia

## ARTICLE INFO

## Article history:

Received 5 August 2021

Received in revised form 4 September 2021

Accepted 8 September 2021

Available online 21 September 2021

## Keywords:

Wettability

Hydrogen geo-storage

Organic acids

Caprock formation

## ABSTRACT

Hydrogen ( $H_2$ ) as a cleaner fuel has been suggested as a viable method of achieving the de-carbonization objectives and meeting increasing global energy demand. However, successful implementation of a full-scale hydrogen economy requires large-scale hydrogen storage (as hydrogen is highly compressible). A potential solution to this challenge is injecting hydrogen into geologic formations from where it can be withdrawn again at later stages for utilization purposes. The geo-storage capacity of a porous formation is a function of its wetting characteristics, which strongly influence residual saturations, fluid flow, rate of injection, rate of withdrawal, and containment security. However, literature severely lacks information on hydrogen wettability in realistic geological and caprock formations, which contain organic matter (due to the prevailing reducing atmosphere). We, therefore, measured advancing ( $\theta_a$ ) and receding ( $\theta_r$ ) contact angles of mica substrates at various representative thermo-physical conditions (pressures 0.1–25 MPa, temperatures 308–343 K, and stearic acid concentrations of  $10^{-9}$  –  $10^{-2}$  mol/L). The mica exhibited an increasing tendency to become weakly water-wet at higher temperatures, lower pressures, and very low stearic acid concentration. However, it turned intermediate-wet at higher pressures, lower temperatures, and increasing stearic acid concentrations. The study suggests that the structural  $H_2$  trapping capacities in geological formations and sealing potentials of caprock highly depend on the specific thermo-physical condition. Thus, this novel data provides a significant advancement in literature and will aid in the implementation of hydrogen geo-storage at an industrial scale.

© 2021 The Authors. Published by Elsevier Ltd. This is an open access article under the CC BY license (<http://creativecommons.org/licenses/by/4.0/>).

## 1. Introduction

The global energy demand is increasing due to the increase in world population and the rapid rate of industrialization (Mohanty et al., 2021). Fossil fuels are the principal source of energy for several sectors of industrialized nations (Heinemann et al., 2021; Lysyy et al., 2021; Nemati et al., 2020; Pan et al., 2021b). However, burning fossil fuels emits large quantities of greenhouse gases,

which leads to climate change (Hashemi et al., 2021a; Heinemann et al., 2021; Yates et al., 2021; Yekta et al., 2018; Zivar et al., 2021). Renewable energy, such as solar power and wind energy, have been explored as feasible alternatives to carbon-based fossil fuels. However, these sources of energy highly depend on atmospheric conditions and specific geographical location (Heinemann et al., 2021; Lin et al., 2021; van der Roest et al., 2020; Yekta et al., 2018). A hydrogen economy is therefore gaining a keen interest as a viable method of achieving the de-carbonization objectives and meeting the increasing energy demand (Gregory and Pangborn, 1976). However, successful implementation of a full-scale hydrogen economy and utilization depends on large-scale hydrogen storage. An effective solution to address this issue is by injecting hydrogen into geo-storage formations and withdrawing it as needed (Ali et al., 2021c; Iglauer et al., 2021b).

\* Corresponding author at: Physical Science and Engineering Division, King Abdullah University of Science and Technology (KAUST), Thuwal, 23955, Saudi Arabia.

\*\* Corresponding author.

E-mail addresses: [Muhammad.ali.2@kaust.edu.sa](mailto:Muhammad.ali.2@kaust.edu.sa),

[Muhammad.ali7@postgrad.curtin.edu.au](mailto:Muhammad.ali7@postgrad.curtin.edu.au) (M. Ali), [Hussein.hoteit@kaust.edu.sa](mailto:Hussein.hoteit@kaust.edu.sa) (H. Hoteit).

Various target formations for H<sub>2</sub> geo-storage have been identified, including depleted hydrocarbon reservoirs, coal beds, high salinity aquifers, tight gas formations, and organic-rich shale reservoirs (Akhondzadeh et al., 2020, 2021; Al-Khdheewi et al., 2021; Dahraj et al., 2016; Liu et al., 2020; Mahesar et al., 2020a,b; Memon et al., 2020; Moradi and Groth, 2019; Ozarslan, 2012; Yekta et al., 2018). Structural, residual, mineral, and dissolution trapping are the four main mechanisms of gas immobilization during geological storage (Iglauer et al., 2015b). Gas can also adsorb onto the surface of organic-rich shale and coal seams, resulting in adsorption trapping (Al-Khdheewi et al., 2020; Ali et al., 2020a; Arif et al., 2021; Iglauer et al., 2021a). However, geo-storage capacities are highly dependent on the wettability and interfacial energies of these formations (Abdullah et al., 2021; Al-Anssari et al., 2018, 2020; Al-Yaseri et al., 2021b; Ali, 2018, 2021; Jha et al., 2018, 2019; Yekeen et al., 2021, 2020). The wettability of rock/H<sub>2</sub>/brine systems influences the pore-scale fluid distribution and dynamics, trapping and storage potentials, as well as the containment security in the storage formations and caprock (Al-Yaseri et al., 2021a; Al-Yaseri and Jha, 2021; Ali et al., 2021c; Iglauer et al., 2021a; Pan et al., 2021a).

Wettability data needed to assess the feasibility of hydrogen storage in geological and caprock formations are very scarce because the concept of hydrogen geo-storage is quite novel (Al-Yaseri and Jha, 2021; Hashemi et al., 2021b; Iglauer et al., 2021b; Pan et al., 2021a). Moreover, laboratory measurement of contact angles of rock/H<sub>2</sub>/brine systems is strenuous due to the high flammability, compressibility, and volatility of hydrogen (Al-Yaseri and Jha, 2021; Ali et al., 2021c; Iglauer et al., 2021b). Thus far, basaltic rock, quartz substrates (sandstone reservoirs), and coal seams have been studied in the literature (Al-Yaseri and Jha, 2021; Ali et al., 2021c; Hashemi et al., 2021b; Iglauer et al., 2021a,b). (Iglauer et al., 2021a) measured the adsorption profiles of H<sub>2</sub> on coal seams, while (Al-Yaseri and Jha, 2021) developed a correlation for estimating the contact angle of H<sub>2</sub> from the contact angles and density of helium, N<sub>2</sub>, and CO<sub>2</sub> measured at 323 K and varying pressures (5–20 MPa). To the best of our knowledge, only (Ali et al., 2021c; Iglauer et al., 2021b), and (Hashemi et al., 2021b) measured the 3-phase contact angles for rock/H<sub>2</sub>/brine systems at high pressure, high temperature (HPHT) conditions for sandstone representative minerals. But these contact angles data do not reveal the wettability and sealing potentials of caprock during large-scale hydrogen geo-storage.

Thus, to assess the sealing potentials of caprock, we measured the advancing and receding contact angles of the mica/H<sub>2</sub>/brine system at realistic reducing (contains organic molecules) and thermo-physical H<sub>2</sub> geo-storage conditions. We then compared the contact angles of mica/H<sub>2</sub>/brine to that of mica/CO<sub>2</sub>/brine and quartz/H<sub>2</sub>/brine systems for validation purposes. Mica is a suitable caprock representative group of minerals due to its ample presence in shales, igneous, metamorphic, and sedimentary rocks (Al-Khdheewi et al., 2020; Ali et al., 2020a; Chiquet et al., 2007; Iglauer et al., 2015a). Thus, the results of this study provide an understanding of the rock wetting phenomenon and potential containment issues associated with H<sub>2</sub> geo-storage, which are crucial knowledge to attain field-scale hydrogen geo-storage.

## 2. Experimental

### 2.1. Materials

The representative caprock mineral used in this study were pristine mica substrates with magnitudes of 14 mm × 12 mm × 2.5 mm = L × W × H. Ward's natural science has provided the rock substrates. The rock surface roughness of pristine mica substrates was measured via Atomic force microscopy (Model

Flex-Axiom, from Nano-surf Company) with an average roughness root mean square of 1 nm. The brine composition was 10 wt% NaCl (prepared by mixing NaCl and deionized water; from David Gray company, with an ultrapure grade, the electrical conductivity of 0.02 mS/cm). Stearic acid (Sigma Aldrich with purity ≥ 98 mol%, details about the stearic acid are provided in Table S1 in the supplementary file) was chosen as the organic acid for the aging of the mica substrates because of their existence geological formations (Ali et al., 2019b, 2020b; Jardine et al., 1989; Stalker et al., 2013).

### 2.2. Methodology

#### 2.2.1. Mica surface cleaning procedure

Initially, deionized water was used to clean the pristine mica substrates to eradicate contaminations on the surface. Thereafter, ultra-pure nitrogen (purity = 99.999% from BOC gas company) was blown on pristine mica substrates followed by drying them at 353 K for 120 min to remove the water film on the surface (Ali et al., 2020a). Finally, the air plasma (Diemer Yocco instrument) treatment procedure (for 20 mins) was implemented for the removal of residual organic molecules (Iglauer et al., 2014; Love et al., 2005).

#### 2.2.2. Aging method for pristine mica substrates

The following procedure was followed to simulate caprock formation over geological times (Davis, 1982; Kleber et al., 2015; Ulrich et al., 1988; Zullig and Morse, 1988): thus, the mica surface was ionized (by exposure to 2 wt% NaCl brine for half an hour at ambient conditions) (Ali et al., 2021a,c, 2020b). Also, the pH of the brine was maintained at 4 by adding droplets of HCl (the concentration of the aqueous hydrochloric acid was 37.5 vol%). These procedures maximize adsorption of the stearic acid on the mica surface (Al-Anssari et al., 2019; Ali et al., 2019a,b; Jardine et al., 1989; Madsen and Ida, 1998; Stalker et al., 2013). Subsequently, the modified mica surfaces were cleaned via blowing with ultra-pure nitrogen to ensure that the residual brine is wiped off from the mica surface. Afterward, brine/HCl ionized mica surfaces were immersed in n-decane/stearic acid solutions (of various concentrations: 10<sup>-2</sup>, 10<sup>-3</sup>, 10<sup>-5</sup>, 10<sup>-7</sup> and 10<sup>-9</sup> mol/L). The mica substrates were left in the stearic acid solutions for 7 days to simulate exposure to formation water for long geo-exposure periods (Ali et al., 2019a,b; Jardine et al., 1989; Madsen and Ida, 1998; Stalker et al., 2013). The wettability of the mica surfaces was thereby changed into strongly hydrophobic (by the stearic acid; Al-Anssari et al., 2016; Ali et al., 2019a,b), also compare schematic S1 in the supplementary material.

#### 2.2.3. Procedure for contact angle measurements

The wettability of mica/H<sub>2</sub>/brine was comprehended by contact angle measurements, a popular method of evaluating the wettability modification characteristics in a particular rock/gas/brine or rock/oil/brine system (Ali et al., 2017, 2015, 2020b; Haghghi et al., 2020; Iglauer et al., 2015a; Nazarhari et al., 2021). Herein, the advancing ( $\theta_a$ ), and receding contact angles ( $\theta_r$ ) were measured via the tilted plate method (Lander et al., 1993). The measurements were carried out at various pressures and elevated temperatures (0.1–25 MPa and 308–343 K), compare also our previous studies about CO<sub>2</sub> (Ali et al., 2020a, 2021a,b). The contact angle values were measured on the acquired images using ImageJ software. The measurements were carried out thrice for every experimental condition, and the mean values of  $\theta_a$  and  $\theta_r$  were computed, based on these replicates, we estimated standard deviations of ± 5° for 25 MPa, and ± 3° for 15 MPa and 0.1 MPa; experiments. The schematic of the experimental setup is shown in Fig. 1. The example contact angle images in the H<sub>2</sub> atmosphere and their associated procedure for calculating advancing and receding contact angles via ImageJ software are presented in the appendix section as Figs. A.1 to A.4.

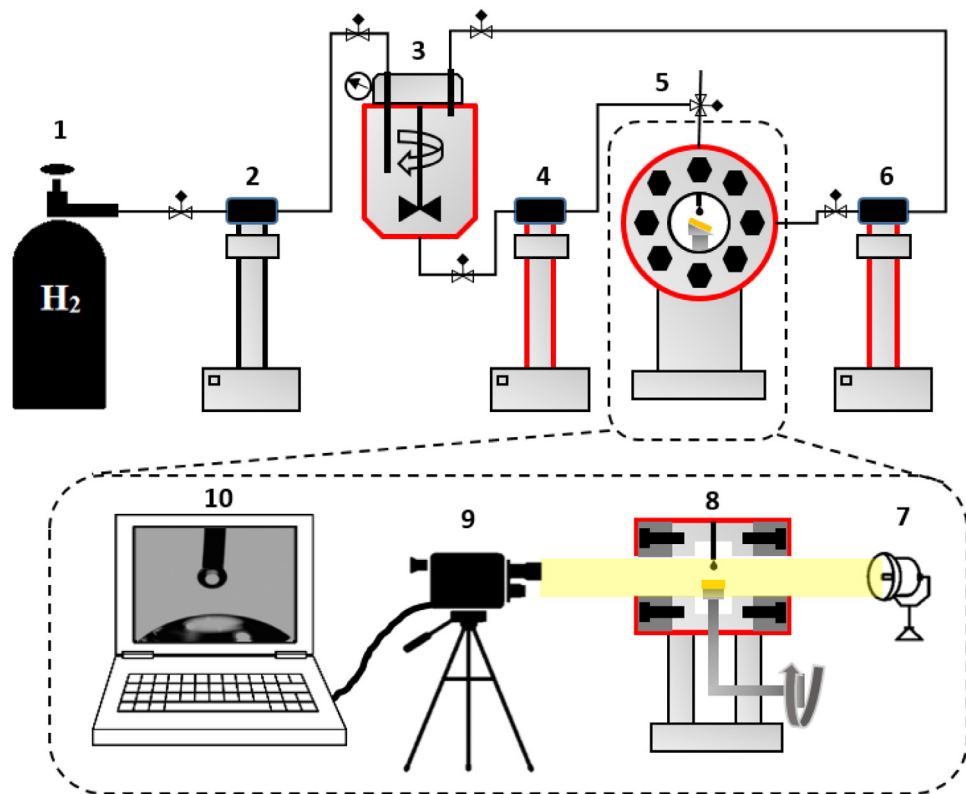


**Fig. 1.** Schematic of the experimental contact angle system (1) H<sub>2</sub> gas bottle, (2) HPHT syringe pump to regulate the H<sub>2</sub> flow, (3) HPHT live brine formulation mixing reactor, (4) HPHT syringe pump to regulate the brine flow, (5) IFT cell made of Hastelloy material having tilted plate inside, front view, (6) HPHT syringe pump for H<sub>2</sub> injection into the cell, (7) Light projection, (8) IFT cell made of Hastelloy material having tilted plate inside, side view, (9) Video camera (high-resolution), (10) Interpretation software (Image).

### 3. Results and discussion

It is essential to assess the impact of H<sub>2</sub> wettability on caprock performance, as caprock is a principal feature guaranteeing to trap (Al-Khdheeawi et al., 2017a,b), and provide containment security (Arif et al., 2016c, 2017; Iglauser et al., 2015a). Herein, the water receding angle ( $\theta_r$ ) is associated with structural trapping capacities when water is displaced by H<sub>2</sub> which is injected into the geo-storage formation (Broseta et al., 2012); capillary leakage could take place when the water receding contact angle is greater than 90° ( $\theta_r > 90^\circ$ ) (Iglauser et al., 2015b). Advancing angle ( $\theta_a$ ) is correlated to residual trapping, at  $\theta_a < 50^\circ$ , when water imbibes again to displace the hydrogen for withdrawal purposes (Al-Menhali and Krevor, 2016; Chiquet et al., 2007; Rahman et al., 2016). All acquired and conducted experimental contact angle data is presented in supplementary file as Tables S2 to S7.

#### 3.1. Impact of temperature and pressure on pure mica/H<sub>2</sub>/brine wettability

Previous studies have shown that the wetting characteristics of rock/CO<sub>2</sub>/brine systems are greatly influenced by temperature (Arif et al., 2016a; Bikikina, 2011; De Ruijter et al., 1998; Iglauser et al., 2012; Pan et al., 2018; Yang et al., 2007), and pressure (Chiquet et al., 2007; Kaveh et al., 2016; Roshan et al., 2016; Saraji et al., 2013; Sarmadivaleh et al., 2015; Siddiqui et al., 2018). This observation demonstrates similarity with the wettability of rock/H<sub>2</sub>/brine systems; e.g. Fig. 2 shows that  $\theta_a$  and  $\theta_r$  increased with increasing pressure. This behavior was caused by the higher molecular gas densities at higher pressures (these enhance the intermolecular interactions between the gas and the solid surfaces (Arif et al., 2016b; Iglauser et al., 2015a)). The increasing pressure,

therefore, promotes the intermolecular interactions between the H<sub>2</sub> gas and the mica substrates. For instance, at 323 K and 5 MPa,  $\theta_a$  and  $\theta_r$  of the pure mica substrates were 21.7° and 18.3°. However, when the pressure was raised to 20 MPa and 323 K,  $\theta_a$  and  $\theta_r$  considerably increased to 42.9° and 36.6°. Similar trends were observed for mica/CO<sub>2</sub>/brine systems, although the degree of contact angles for CO<sub>2</sub> systems are generally always higher. For instance, at 323 K and 5 MPa,  $\theta_a$  and  $\theta_r$  of the mica/CO<sub>2</sub>/brine system were 39.1° and 30.5° respectively, whereas, at 20 MPa and 323 K,  $\theta_a$  and  $\theta_r$  rose to 83.5° and 74.2°. The lower H<sub>2</sub>/mica contact angles compared to that of the CO<sub>2</sub>/mica system can be attributed to the lower density of the H<sub>2</sub> (compared to CO<sub>2</sub> at the same temperature and pressure; (Al-Yaseri and Jha, 2021; Ali et al., 2021c; Hashemi et al., 2021b; Iglauser et al., 2021a,b)). For instance, at 323 K and 25 MPa, hydrogen and CO<sub>2</sub> densities are 16.4 kg/m<sup>3</sup> and 834.9 kg/m<sup>3</sup>, respectively (Iglauser et al., 2021b; Leachman et al., 2009; Span and Wagner, 1996).

Fig. 2 also shows that mica/H<sub>2</sub>/brine contact angles decreased with increasing temperature, suggesting that the sealing capacity of warmer reservoirs is higher; for instance, at 15 MPa,  $\theta_a$  and  $\theta_r$  were 53.1° and 47.3° at 308 K compared to 35.4° and 29.2° at 343 K, respectively (the similar trend was observed for CO<sub>2</sub>, but the degree of change was higher than H<sub>2</sub>). This observation can be explained by the reduction in H<sub>2</sub> gas density with increasing temperature. For instance, when the temperature was raised to 343 K (at 25 MPa), hydrogen and CO<sub>2</sub> density decreased to 15.5 kg/m<sup>3</sup> and 737.7 kg/m<sup>3</sup>, respectively (Iglauser et al., 2021b; Leachman et al., 2009; Span and Wagner, 1996).

H<sub>2</sub> gas density decreases at high temperatures because the molecular cohesive energy density of H<sub>2</sub> is lower at higher temperatures. As the molecules of the H<sub>2</sub> gas are heated up, they gain kinetic energy and move faster, leading to higher collision

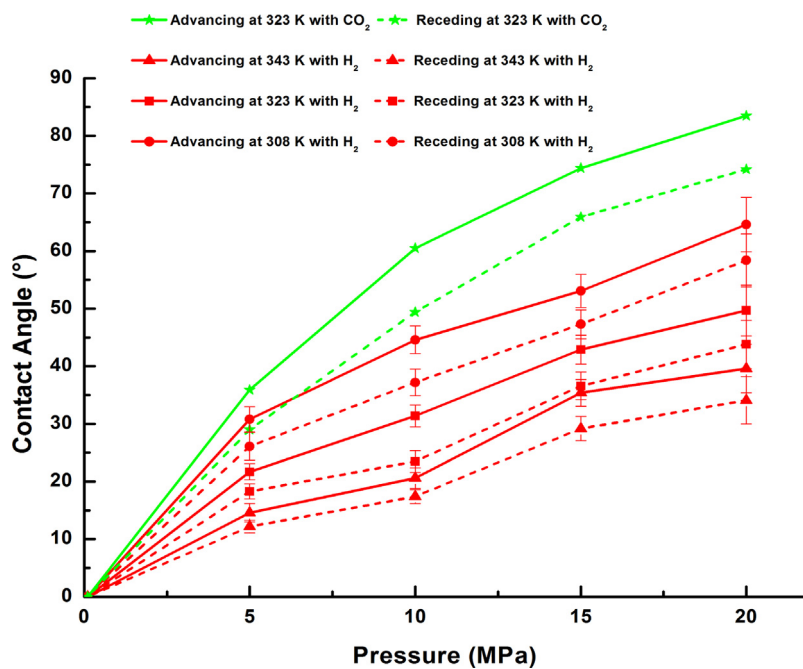


**Fig. 2.** Advancing and receding contact angle data on pure mica/H<sub>2</sub>/brine systems as a function of pressure and temperature, shown with red lines. Green lines depict the advancing and receding contact angle data as a function of pressure for pure mica/CO<sub>2</sub>/brine systems.. (For interpretation of the references to color in this figure legend, the reader is referred to the web version of this article.)

Source: The pure mica/CO<sub>2</sub>/brine data is taken from Arif et al. (2016a).

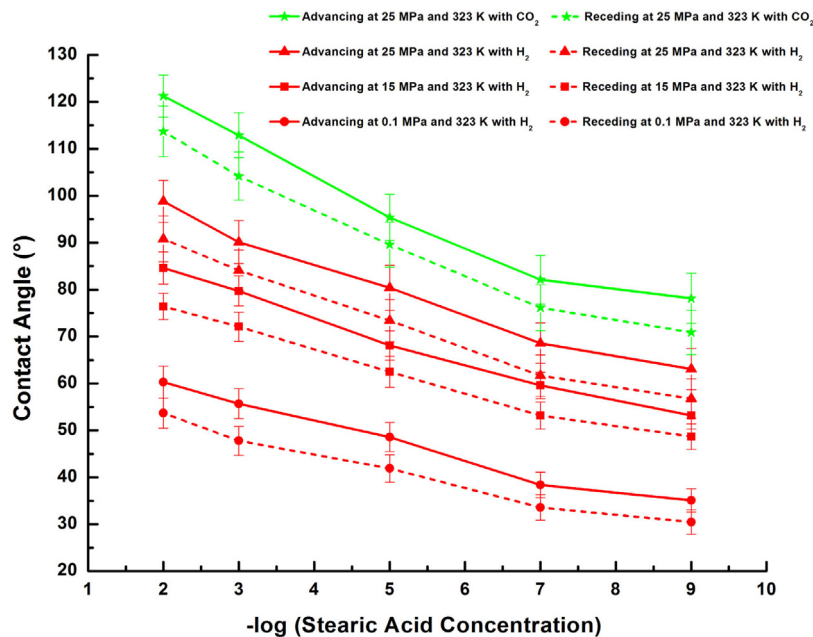


**Fig. 3.** Advancing and receding contact angle data on mica/H<sub>2</sub>/brine systems as a function of stearic acid concentration (mol/L); red lines. Green lines depict the contact angle (advancing and receding) data on mica/CO<sub>2</sub>/brine systems as a function of stearic acid concentration (mol/L).. (For interpretation of the references to color in this figure legend, the reader is referred to the web version of this article.)

Source: The organic-aged mica/CO<sub>2</sub>/brine data is taken from Ali et al. (2020a).

and accelerated diffusion; this reduces the molecular interactions between the mica surface and H<sub>2</sub>, thus the contact angle reduces with increasing temperature.

### 3.2. Influence of organic acid concentration on mica/H<sub>2</sub>/brine wetability

A typical caprock acts as an effective seal; the caprock is therefore ideally strongly water-wet, to optimally restrict upward

migration of H<sub>2</sub>. Indeed, whenever  $\theta_r > 90^\circ$  (H<sub>2</sub>-wet condition), H<sub>2</sub> can migrate into the caprock, interact in unknown ways with the caprock, and percolate upwards through the caprock, resulting in a higher risk of leakage (Ali et al., 2020a; Iglauer et al., 2015a,b). The structural trapping capacities of caprock can thus be greatly influenced by organic acid contamination presence on the rock surfaces (Ali et al., 2020a, 2019a, 2021b,c). Experiments conducted with pure mica, when the effects of organic contaminations on rock surfaces were not considered, showed that

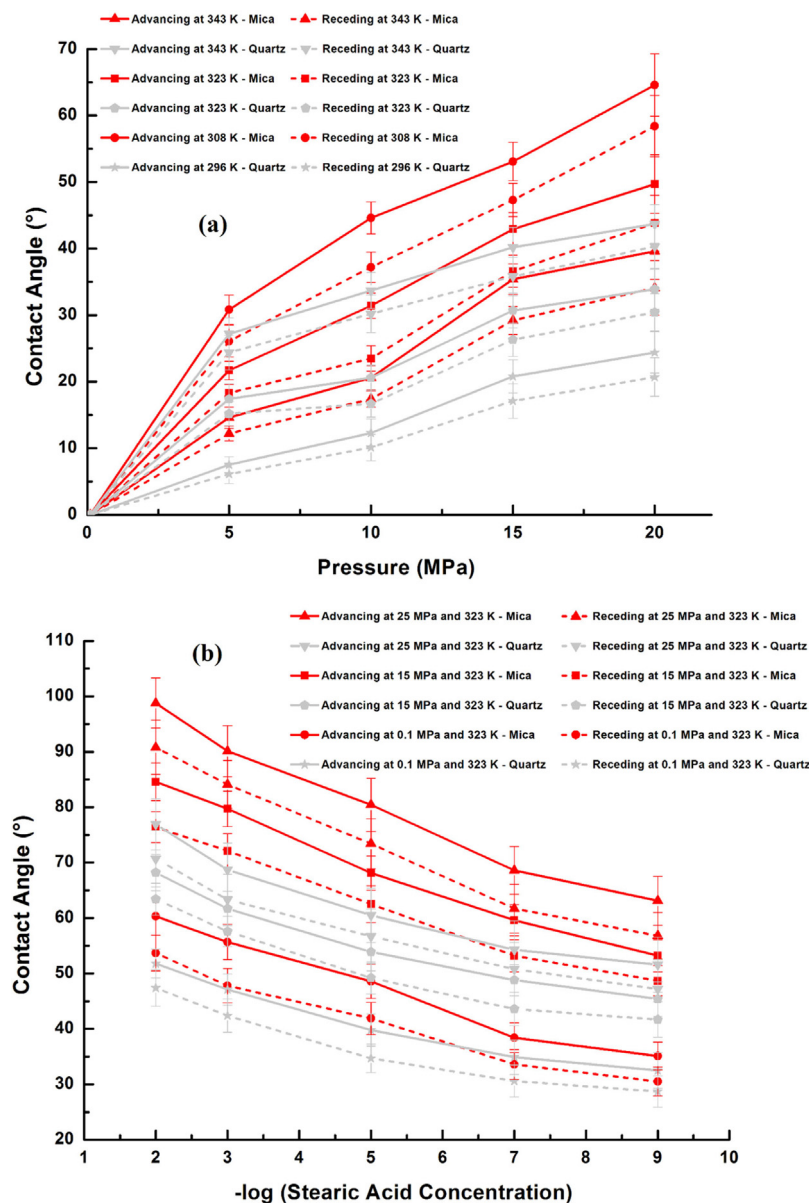


**Fig. 4.** (a) Advancing and receding contact angles data of pure mica/H<sub>2</sub>/brine (red lines) and pure quartz/H<sub>2</sub>/brine (gray lines) systems as a function of varying pressure and temperature, (b) Advancing and receding contact angles data of mica/H<sub>2</sub>/brine (red lines) and quartz/H<sub>2</sub>/brine (gray lines) systems as a function of stearic acid concentration (mol/L). (For interpretation of the references to color in this figure legend, the reader is referred to the web version of this article.) Source: The pure and organic-aged quartz/H<sub>2</sub>/brine data is taken from Iglauer et al. (2021b).

the mica substrates remained strongly water-wet at high temperature and weakly-water wet at low-temperature conditions. However, higher contact angles were measured for mica/H<sub>2</sub>/brine systems when the mica substrates were aged in different concentrations of stearic acid. Fig. 3 clearly shows that at constant temperature (323 K), the hydrogen wettability of mica increased with increasing organic acid concentration and pressure. For instance, at 15 MPa and 323 K,  $\theta_a$  and  $\theta_r$  increased from 53.2° and 48.7° to 84.6° and 76.4°, respectively, when the concentration of stearic acid increased from  $10^{-9}$  mol/L to  $10^{-2}$  mol/L. Even minute stearic acid concentration of  $10^{-9}$  mol/L, at 15 MPa, and 323 K had a significant impact on contact angle ( $\theta_a = 53.2^\circ$  and  $\theta_r = 48.7^\circ$  vs.  $\theta_a = 42.9^\circ$  and  $\theta_r = 36.6^\circ$  for pure mica). However, at higher pressures, this degree of change was higher. For example, at 25 MPa, 323 K, and  $10^{-2}$  mol/L stearic acid concentration, the hydrogen-mica wettability attained hydrogen-wet conditions ( $\theta_a = 98.8^\circ$  and  $\theta_r = 90.8^\circ$ ). Such alteration of caprock wettability to hydrogen-wet conditions ( $\theta_r > 90^\circ$ ) could

decrease the structural trapping potentials of caprock formation, resulting in a higher risk of caprock leakage during hydrogen geological storage (Ali et al., 2021c; Iglauer et al., 2021b).

A comparison of H<sub>2</sub>-wettability to CO<sub>2</sub>-wettability of mica showed similar trends in contact angles changes with varying pressure and stearic acid concentration (Fig. 3). However, the alterations in contact angles were much more significant for mica/CO<sub>2</sub>/brine compared to the mica/H<sub>2</sub>/brine system, which is due to higher molecular densities of CO<sub>2</sub> compared to H<sub>2</sub>. These results confirm that the hydrogen-wettability of a particular caprock formation is less than the CO<sub>2</sub>-wettability of such rocks at similar conditions, suggesting that the structural trapping mechanism of caprock is lower during CO<sub>2</sub> geo-storage compared to H<sub>2</sub> geo-storage (Al-Yaseri and Jha, 2021; Ali et al., 2021c; Hashemi et al., 2021b; Iglauer et al., 2021a,b). Nevertheless, the overall leakage risk of H<sub>2</sub> remains higher compared to CO<sub>2</sub> because of its higher mobility and lower density.

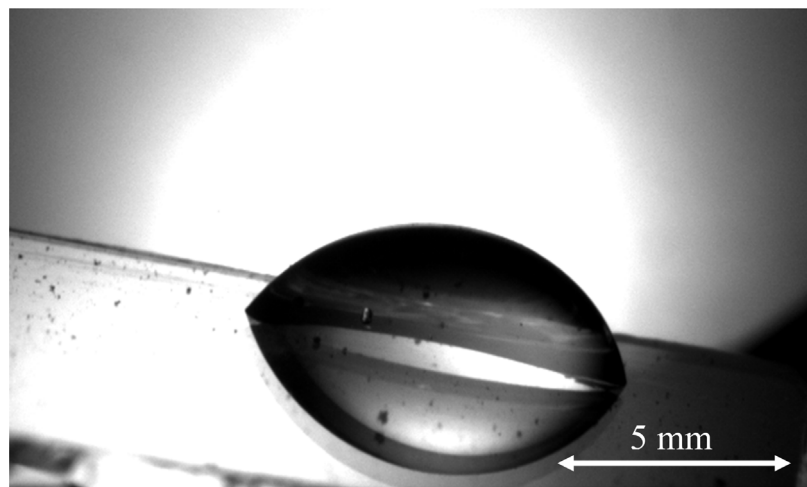


**Fig. A.1.** Contact angle image (pure mica, 20 MPa, and 308 K), the brine drop (dark) sits on the mica surface (gray) in the H<sub>2</sub> atmosphere (transparent/white).

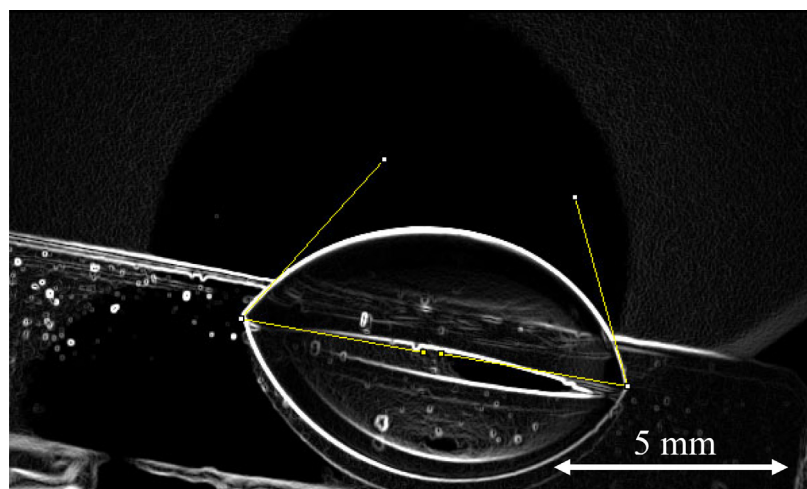


**Fig. A.2.** ImageJ experimental measurements of advancing contact angle ( $\sim 64.6^\circ$ ) at the leading edge and receding contact angle ( $\sim 58.4^\circ$ ) at the trailing edge of droplet for [Fig. A.1](#).

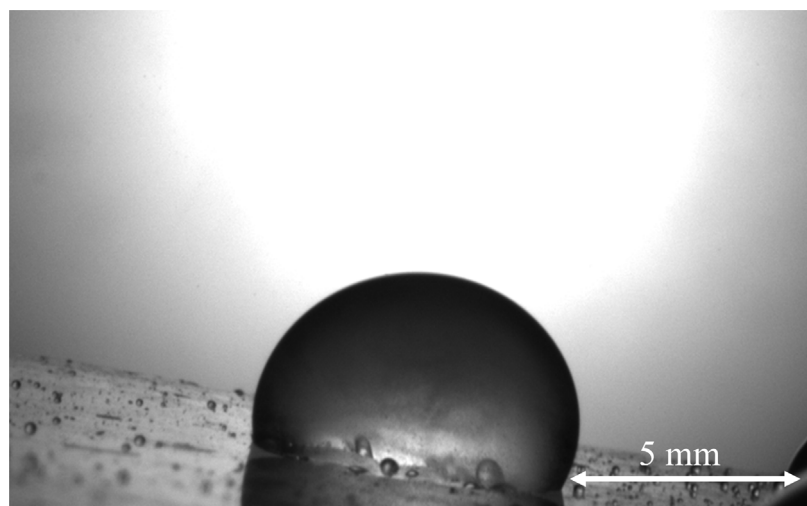


**Fig. A.3.** Contact angle image ( $10^{-2}$  mol/L stearic acid concentration, 25 MPa, and 323 K), the brine drop (dark) sits on the mica surface (gray) in the H<sub>2</sub> atmosphere (transparent/white).

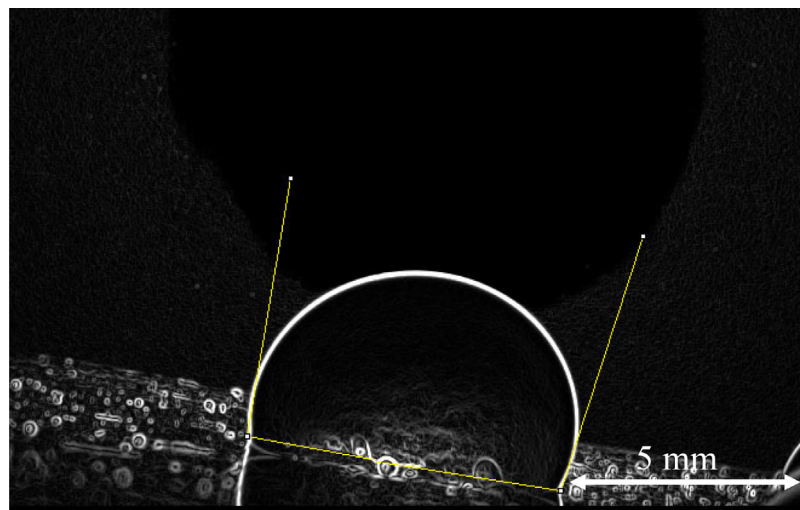


**Fig. A.4.** Imagej experimental measurements of advancing contact angle ( $\sim 98.8^\circ$ ) at the leading edge and receding contact angle ( $\sim 90.8^\circ$ ) at the trailing edge of droplet for Fig. A.3.

### 3.3. Comparison of mica/H<sub>2</sub>/brine and quartz/H<sub>2</sub>/brine systems

Comparisons between the wetting characteristics of pure mica/H<sub>2</sub>/brine and pure quartz/H<sub>2</sub>/brine systems (Fig. 4a) depict that the contact angles of both systems were higher at high pressures; however, the temperature effects on both systems were dissimilar. Contact angles of the mica/H<sub>2</sub>/brine decreased with increasing temperature, while quartz/H<sub>2</sub>/brine contact angles increased with temperature. These results are consistent with the literature on rock/CO<sub>2</sub>/brine systems (Arif et al., 2016a; Sarmadivaleh et al., 2015). Previous research emphasized that quartz/H<sub>2</sub>/brine contact angles were higher at elevated temperatures because of the tendency of hydrogen bonds (between the quartz surface, silanol groups, and the molecules of water) to be broken at high temperatures. This phenomenon increased the propensity of the quartz surface to become water de-wetted at high temperatures (Ali et al., 2021c; Hashemi et al., 2021b; Iglaue et al., 2021b). The mica/H<sub>2</sub>/brine contact angles were lower at high temperature due to the decreased hydrogen density at a higher temperature, suggesting that the contact angles of mica/H<sub>2</sub>/brine greatly depend on H<sub>2</sub> density instead of hydrogen bonding (Al-Yaseri et al., 2016; Zivar et al., 2020). For instance, at 343 K and 20 MPa, in pure quartz/H<sub>2</sub>/brine systems,  $\theta_a$  was 43.7°, and  $\theta_r$  was 40.3°, while  $\theta_a$  was 39.6°, and  $\theta_r = 34.1^\circ$  for pure mica/H<sub>2</sub>/brine systems.

A comparison of the effects of organic contamination on the wettability of mica/H<sub>2</sub>/brine and quartz/H<sub>2</sub>/brine systems is presented in Fig. 4b. The results suggest that similar to mica,  $\theta_a$  and  $\theta_r$  were higher when the quartz substrates were aged in different concentrations of stearic acid ( $10^{-9}$  mol/L– $10^{-2}$  mol/L). However, at similar pressure and temperature conditions, the mica–hydrogen contact angles were significantly higher compared to quartz–hydrogen contact angles. For instance, at 323 K and 25 MPa, the mica–H<sub>2</sub> turned hydrogen-wet (with  $\theta_a = 98.8^\circ$  and  $\theta_r = 90.8^\circ$ ) when the rock was aged in  $10^{-2}$  mol/L stearic acid concentration. However, at similar thermo-physical conditions and stearic acid concentration, the quartz–H<sub>2</sub> attained intermediate wetting condition (with  $\theta_a = 76.9^\circ$  and  $\theta_r = 70.7^\circ$ ). It is clear from these results that in the presence of organic contaminations, surfaces with high initial hydrophilic sites, such as quartz, are expected to have lower rock–hydrogen contact angles and significantly higher rock/H<sub>2</sub> interfacial energies compared to surfaces with originally less hydrophilic sites (such as mica and calcite). It can be inferred from the results of this study that large-scale

storage of H<sub>2</sub> could be considerably affected by even the minute concentrations of organic acid. Thus, the structural/stratigraphic trapping potential of caprock formations and residual trapping capacities of sandstone formations at realistic H<sub>2</sub> geo-storage conditions will be substantially lower than expected. Moreover, the CO<sub>2</sub> wettability of mica was higher than the H<sub>2</sub> wettability of mica at all conditions investigated in this study, suggesting that the CO<sub>2</sub> gas could be used as cushion gas for the maintenance of formation pressure during hydrogen storage and extraction. This will permit easier disarticulation, as well as withdrawal of hydrogen during the injection/production process (Al-Yaseri and Jha, 2021; Zivar et al., 2020). Hence, it can be concluded that large-scale storage of hydrogen will be favorable in storage and caprock formations with significantly lower surface energies in the presence of organic acids.

### 4. Conclusions

As part of the recent quest for the successful implementation of a hydrogen economy (Heinemann et al., 2021; Lin et al., 2021; van der Roest et al., 2020; Yekta et al., 2018), this study was conducted to provide insight into the possibility of large scale H<sub>2</sub> storage in geological formation and specifically the assessment of the sealing capacities of associated caprocks. The reported data on hydrogen wettability for geo-storage formations is quite scarce. Therefore, contact angles of mica/H<sub>2</sub>/brine systems were measured through the tilted plate method, at representative geo-storage temperature (308–343 K), pressures (0.1–25 MPa), and various stearic acid concentrations ( $10^{-9}$  –  $10^{-2}$  mol/L). Contact angles of mica/H<sub>2</sub>/brine were then compared with that of mica/CO<sub>2</sub>/brine and quartz/H<sub>2</sub>/brine systems to further assess the structural and residual trapping potentials of H<sub>2</sub>. The mica demonstrated an increasing tendency to become weakly water-wet at high pressure and low temperature and intermediate-wet with increasing stearic acid concentrations.

For instance, pure mica at 323 K and 20 MPa, mica/H<sub>2</sub>/brine contact angles were at weakly water-wet conditions ( $\theta_a = 49.7^\circ$  and  $\theta_r = 43.8^\circ$ ), whereas mica/CO<sub>2</sub>/brine contact angles were at intermediate-wet conditions ( $\theta_a = 83.5^\circ$  and  $\theta_r = 74.2^\circ$ ). In the presence of  $10^{-2}$  mol/L stearic acid at 323 K and 25 MPa, mica/H<sub>2</sub>/brine system became hydrogen-wet ( $\theta_a = 98.8^\circ$  and  $\theta_r = 90.8^\circ$ ), while quartz/H<sub>2</sub>/brine remained intermediate-wet ( $\theta_a = 76.9^\circ$  and  $\theta_r = 70.7^\circ$ ) from initial strongly water-wet conditions ( $\theta_a = 40.8^\circ$  and  $\theta_r = 35.1^\circ$ ). These results suggest that

caprocks are efficient in terms of hydrogen storage from a wettability perspective. However, the effects of organic acids should be accounted for to ensure successful and safe industrial-scale hydrogen storage.

## CRediT authorship contribution statement

**Muhammad Ali:** Conceptualization, Methodology, Validation, Formal analysis, Investigation, Data curation, Writing – original draft, Writing – review & editing. **Nurudeen Yekeen:** Visualization, Writing – review & editing. **Nilanjan Pal:** Data curation, Methodology. **Alireza Keshavarz:** Software, Validation. **Stefan Iglauer:** Validation, Writing – review & editing. **Hussein Hoteit:** Resources, Writing – review & editing, Project administration, Supervision.

## Declaration of competing interest

The authors declare that they have no known competing financial interests or personal relationships that could have appeared to influence the work reported in this paper.

## Appendix A

See Figs. A.1–A.4.

## Appendix B. Supplementary data

Supplementary material related to this article can be found online at <https://doi.org/10.1016/j.egyr.2021.09.016>.

## References

- Abdullah, H., et al., 2021. CO<sub>2</sub>/basalt's interfacial tension and wettability directly from gas density: Implications for carbon geo-sequestration. *J. Pet. Sci. Eng.* 108683.
- Akhondzadeh, H., et al., 2020. Pore-scale analysis of coal cleat network evolution through liquid nitrogen treatment: A micro-computed tomography investigation. *Int. J. Coal Geol.* 219, 103370.
- Akhondzadeh, H., et al., 2021. Liquid nitrogen fracturing efficiency as a function of coal rank: A multi-scale tomographic study. *J. Nat. Gas Sci. Eng.* 104177.
- Al-Ansari, S., Barifcany, A., Wang, S., Maxim, L., Iglauer, S., 2016. Wettability alteration of oil-wet carbonate by silica nanofluid. *J. Colloid Interface Sci.* 461, 435–442.
- Al-Ansari, S., et al., 2018. Influence of pressure and temperature on CO<sub>2</sub>-nanofluid interfacial tension: Implication for enhanced oil recovery and carbon geosequestration. In: Abu Dhabi International Petroleum Exhibition & Conference. Society of Petroleum Engineers.
- Al-Ansari, S., et al., 2019. Reversible and irreversible adsorption of bare and hybrid silica nanoparticles onto carbonate surface at reservoir condition. *Petroleum*.
- Al-Ansari, S., et al., 2020. Effect of nanoparticles on the interfacial tension of CO<sub>2</sub>-oil system at high pressure and temperature: An experimental approach. In: SPE Asia Pacific Oil & Gas Conference and Exhibition. Society of Petroleum Engineers.
- Al-Khdheeawi, E.A., Mahdi, D.S., Ali, M., Fauziah, C.A., Barifcany, A., 2020. Impact of caprock type on geochemical reactivity and mineral trapping efficiency of CO<sub>2</sub>. In: Offshore Technology Conference Asia. OnePetro.
- Al-Khdheeawi, E.A., Mahdi, D.S., Ali, M., Iglauer, S., Barifcany, A., 2021. Reservoir scale porosity-permeability evolution in sandstone due to CO<sub>2</sub> geological storage. Available at SSRN 3818887.
- Al-Khdheeawi, E.A., Vialle, S., Barifcany, A., Sarmadivaleh, M., Iglauer, S., 2017a. Impact of reservoir wettability and heterogeneity on CO<sub>2</sub>-plume migration and trapping capacity. *Int. J. Greenh. Gas Control* 58, 142–158.
- Al-Khdheeawi, E.A., Vialle, S., Barifcany, A., Sarmadivaleh, M., Iglauer, S., 2017b. Influence of injection well configuration and rock wettability on CO<sub>2</sub> plume behaviour and CO<sub>2</sub> trapping capacity in heterogeneous reservoirs. *J. Nat. Gas Sci. Eng.* 43, 190–206.
- Al-Menhal, A.S., Krevor, S., 2016. Capillary trapping of CO<sub>2</sub> in oil reservoirs: Observations in a mixed-wet carbonate rock. *Environ. Sci. Technol.* 50 (5), 2727–2734.
- Al-Yaseri, A., Ali, M., Ali, M., Taheri, R., Wolff-Boenisch, D., 2021b. Western Australia basalt-CO<sub>2</sub>-brine wettability at geo-storage conditions. *J. Colloid Interface Sci.*
- Al-Yaseri, A., Jha, N.K., 2021. On hydrogen wettability of basaltic rock. *J. Pet. Sci. Eng.* 200, 108387.
- Al-Yaseri, A.Z., Roshan, H., Lebedev, M., Barifcany, A., Iglauer, S., 2016. Dependence of quartz wettability on fluid density. *Geophys. Res. Lett.* 43 (8), 3771–3776.
- Al-Yaseri, A., et al., 2021a. Assessment of CO<sub>2</sub>/shale interfacial tension. *Colloids Surf. A* 127118.
- Ali, M., 2018. Effect of Organic Surface Concentration on CO<sub>2</sub>-Wettability of Reservoir Rock. Curtin University.
- Ali, M., 2021. Effect of Organics and Nanoparticles on CO<sub>2</sub>-Wettability of Reservoir Rock; Implications for CO<sub>2</sub> Geo-Storage. Curtin University.
- Ali, M., Dahraj, N.U., Haider, S.A., 2015. Study of asphaltene precipitation during CO<sub>2</sub> injection in light oil reservoirs. In: SPE/PAPG Pakistan Section Annual Technical Conference. Society of Petroleum Engineers.
- Ali, M., et al., 2017. Influence of miscible CO<sub>2</sub> flooding on wettability and asphaltene precipitation in Indiana lime stone. In: SPE/IATMI Asia Pacific Oil & Gas Conference and Exhibition. Society of Petroleum Engineers.
- Ali, M., et al., 2019a. Organic acid concentration thresholds for ageing of carbonate minerals: Implications for CO<sub>2</sub> trapping/storage. *J. Colloid Interface Sci.* 534, 88–94.
- Ali, M., et al., 2019b. CO<sub>2</sub>-wettability of sandstones exposed to traces of organic acids: Implications for CO<sub>2</sub> geo-storage. *Int. J. Greenh. Gas Control* 83, 61–68.
- Ali, M., et al., 2020a. Influence of organic acid concentration on wettability alteration of cap-rock: Implications for CO<sub>2</sub> trapping/storage. *ACS Appl. Mater. Interfaces* 12 (35), 39850–39858.
- Ali, M., et al., 2020b. Effect of nanofluid on CO<sub>2</sub>-wettability reversal of sandstone formation; implications for CO<sub>2</sub> geo-storage. *J. Colloid Interface Sci.* 559, 304–312.
- Ali, M., et al., 2021a. CO<sub>2</sub>-wettability reversal of cap-rock by alumina nanofluid: Implications for CO<sub>2</sub> geo-storage. *Fuel Process. Technol.* 214, 106722.
- Ali, M., et al., 2021b. Effect of humic acid on CO<sub>2</sub>-wettability in sandstone formation. *J. Colloid Interface Sci.* 588, 315–325.
- Ali, M., et al., 2021c. Hydrogen wettability of quartz substrates exposed to organic acids: Implications for hydrogen trapping/storage in sandstone reservoirs. *J. Pet. Sci. Eng.* 109081.
- Arif, M., Al-Yaseri, A.Z., Barifcany, A., Lebedev, M., Iglauer, S., 2016a. Impact of pressure and temperature on CO<sub>2</sub>-brine-mica contact angles and CO<sub>2</sub>-brine interfacial tension: Implications for carbon geo-sequestration. *J. Colloid Interface Sci.* 462, 208–215.
- Arif, M., Barifcany, A., Lebedev, M., Iglauer, S., 2016b. CO<sub>2</sub> wettability of shales and coals as a function of pressure, temperature and rank: Implications for CO<sub>2</sub> sequestration and enhanced methane recovery. In: PAPG/SPE Pakistan Section Annual Technical Conference and Exhibition. Society of Petroleum Engineers.
- Arif, M., Barifcany, A., Lebedev, M., Iglauer, S., 2016c. Structural trapping capacity of oil-wet caprock as a function of pressure, temperature and salinity. *Int. J. Greenh. Gas Control* 50, 112–120.
- Arif, M., Lebedev, M., Barifcany, A., Iglauer, S., 2017. Influence of shale-total organic content on CO<sub>2</sub> geo-storage potential. *Geophys. Res. Lett.* 44 (17), 8769–8775.
- Arif, M., Zhang, Y., Iglauer, S., 2021. Shale wettability: Data sets, challenges, and outlook. *Energy Fuels* 35 (4), 2965–2980.
- Bikkina, P.K., 2011. Contact angle measurements of CO<sub>2</sub>-water-quartz/calcite systems in the perspective of carbon sequestration. *Int. J. Greenh. Gas Control* 5 (5), 1259–1271.
- Broseta, D., Tonnet, N., Shah, V., 2012. Are rocks still water-wet in the presence of dense CO<sub>2</sub> or H<sub>2</sub>S? *Geofluids* 12 (4), 280–294.
- Chiquet, P., Broseta, D., Thibeau, S., 2007. Wettability alteration of caprock minerals by carbon dioxide. *Geofluids* 7 (2), 112–122.
- Dahraj, N.U., Ali, M., Khan, M.N., 2016. End of linear flow time picking in long transient hydraulically fractured wells to correctly estimate the permeability, fracture half-length and original gas in place in liquid rich shales. In: PAPG/SPE Pakistan Section Annual Technical Conference and Exhibition. Society of Petroleum Engineers.
- Davis, J.A., 1982. Adsorption of natural dissolved organic matter at the oxide/water interface. *Geochim. Cosmochim. Acta* 46 (11), 2381–2393.
- De Ruijter, M., Kölsch, P., Voué, M., De Coninck, J., Rabe, J., 1998. Effect of temperature on the dynamic contact angle. *Colloids Surf. A* 144 (1–3), 235–243.
- Gregory, D.P., Pangborn, J., 1976. Hydrogen energy. *Annu. Rev. Energy* 1 (1), 279–310.
- Haghghi, O.M., et al., 2020. Effect of environment-friendly non-ionic surfactant on interfacial tension reduction and wettability alteration; implications for enhanced oil recovery. *Energies* 13 (15), 3988.
- Hashemi, L., Blunt, M., Hajibeygi, H., 2021a. Pore-scale modelling and sensitivity analyses of hydrogen-brine multiphase flow in geological porous media. *Sci. Rep.* 11 (1), 1–13.
- Hashemi, L., Glerum, W., Farajzadeh, R., Hajibeygi, H., 2021b. Contact angle measurement for hydrogen/brine/sandstone system using captive-bubble method relevant for underground hydrogen storage. *Adv. Water Resour.* 103964.

- Heinemann, N., et al., 2021. Enabling large-scale hydrogen storage in porous media—the scientific challenges. *Energy Environ. Sci.* 14 (2), 853–864.
- Iglauer, S., Abid, H., Al-Yaseri, A., Keshavarz, A., 2021a. Hydrogen adsorption on sub-bituminous coal: Implications for hydrogen geo-storage. *Geophys. Res. Lett.* 48 (10), e2021GL092976.
- Iglauer, S., Al-Yaseri, A.Z., Rezaee, R., Lebedev, M., 2015a. CO<sub>2</sub> wettability of caprocks: Implications for structural storage capacity and containment security. *Geophys. Res. Lett.* 42 (21), 9279–9284.
- Iglauer, S., Ali, M., Keshavarz, A., 2021b. Hydrogen wettability of sandstone reservoirs: Implications for hydrogen geo-storage. *Geophys. Res. Lett.* 48 (3), 1–5.
- Iglauer, S., Mathew, M., Bresme, F., 2012. Molecular dynamics computations of brine–CO<sub>2</sub> interfacial tensions and brine–CO<sub>2</sub>–quartz contact angles and their effects on structural and residual trapping mechanisms in carbon geo-sequestration. *J. Colloid Interface Sci.* 386 (1), 405–414.
- Iglauer, S., Pentland, C., Busch, A., 2015b. CO<sub>2</sub> wettability of seal and reservoir rocks and the implications for carbon geo-sequestration. *Water Resour. Res.* 51 (1), 729–774.
- Iglauer, S., Salama, A., Sarmadivaleh, M., Liu, K., Phan, C., 2014. Contamination of silica surfaces: Impact on water–CO<sub>2</sub>–quartz and glass contact angle measurements. *Int. J. Greenh. Gas Control* 22, 325–328.
- Jardine, P., McCarthy, J., Weber, N., 1989. Mechanisms of dissolved organic carbon adsorption on soil. *Soil Sci. Am. J.* 53 (5), 1378–1385.
- Jha, N., et al., 2018. Low salinity surfactant nanofluids for enhanced CO<sub>2</sub> storage application at high pressure and temperature. In: Fifth CO<sub>2</sub> Geological Storage Workshop. European Association of Geoscientists & Engineers, pp. 1–4.
- Jha, N.K., et al., 2019. Wettability alteration of quartz surface by low-salinity surfactant nanofluids at high-pressure and high-temperature conditions. *Energy Fuels* 33 (8), 7062–7068.
- Kaveh, N.S., Barnhoorn, A., Wolf, K.-H., 2016. Wettability evaluation of silty shale caprocks for CO<sub>2</sub> storage. *Int. J. Greenh. Gas Control* 49, 425–435.
- Kleber, M., et al., 2015. Mineral–organic associations: formation, properties, and relevance in soil environments. In: *Advances in Agronomy*. Elsevier, pp. 1–140.
- Lander, L.M., Siewierski, L.M., Brittain, W.J., Vogler, E.A., 1993. A systematic comparison of contact angle methods. *Langmuir* 9 (8), 2237–2239.
- Leachman, J.W., Jacobsen, R.T., Penoncello, S., Lemmon, E.W., 2009. Fundamental equations of state for parahydrogen, normal hydrogen, and orthohydrogen. *J. Phys. Chem. Ref. Data* 38 (3), 721–748.
- Lin, H., et al., 2021. Economic and technological feasibility of using power-to-hydrogen technology under higher wind penetration in China. *Renew. Energy* 173, 569–580.
- Li, W., et al., 2020. Feasibility evaluation of large-scale underground hydrogen storage in bedded salt rocks of China: A case study in Jiangsu province. *Energy* 198, 117348.
- Love, J.C., Estroff, L.A., Kriebel, J.K., Nuzzo, R.G., Whitesides, G.M., 2005. Self-assembled monolayers of thiolates on metals as a form of nanotechnology. *Chem. Rev.* 105 (4), 1103–1170.
- Lysyy, M., Ferno, M., Ersland, G., 2021. Seasonal hydrogen storage in a depleted oil and gas field. *Int. J. Hydrogen Energy*.
- Madsen, L., Ida, L., 1998. Adsorption of carboxylic acids on reservoir minerals from organic and aqueous phase. *SPE Reserv. Eval. Eng.* 1 (01), 47–51.
- Mahesar, A.A., et al., 2020a. Effect of cryogenic liquid nitrogen on the morphological and petrophysical characteristics of tight gas sandstone rocks from Kirthar fold belt, Indus Basin, Pakistan. *Energy Fuels* 34 (11), 14548–14559.
- Mahesar, A.A., et al., 2020b. Morphological and petro physical estimation of eocene tight carbonate formation cracking by cryogenic liquid nitrogen; a case study of Lower Indus basin, Pakistan. *J. Pet. Sci. Eng.* 107318.
- Memon, K.R., et al., 2020. Influence of cryogenic liquid nitrogen on petro-physical characteristics of mancos shale: An experimental investigation. *Energy Fuels* 34 (2), 2160–2168.
- Mohanty, U.S., et al., 2021. Current advances in syngas (CO+ H<sub>2</sub>) production through bi-reforming of methane using various catalysts: A review. *Int. J. Hydrogen Energy*.
- Moradi, R., Groth, K.M., 2019. Hydrogen storage and delivery: Review of the state of the art technologies and risk and reliability analysis. *Int. J. Hydrogen Energy* 44 (23), 12254–12269.
- Nazarahari, M.J., et al., 2021. Impact of a novel biosynthesized nanocomposite (SiO<sub>2</sub>@ Montmorillonite@ Xanthan) on wettability shift and interfacial tension: Applications for enhanced oil recovery. *Fuel* 298, 120773.
- Nemati, B., et al., 2020. A sustainable approach for site selection of underground hydrogen storage facilities using fuzzy-delphi methodology. *Settl. Spat. Plan.* 6, 5–16.
- Ozarslan, A., 2012. Large-scale hydrogen energy storage in salt caverns. *Int. J. Hydrogen Energy* 37 (19), 14265–14277.
- Pan, B., Li, Y., Wang, H., Jones, F., Iglauer, S., 2018. CO<sub>2</sub> and CH<sub>4</sub> wettabilities of organic-rich shale. *Energy Fuels* 32 (2), 1914–1922.
- Pan, B., Yin, X., Iglauer, S., 2021a. Rock-fluid interfacial tension at subsurface conditions: Implications for H<sub>2</sub>, CO<sub>2</sub> and natural gas geo-storage. *Int. J. Hydrogen Energy*.
- Pan, B., Yin, X., Ju, Y., Iglauer, S., 2021b. Underground hydrogen storage: Influencing parameters and future outlook. *Adv. Colloid Interface Sci.* 102473.
- Rahman, T., Lebedev, M., Barifcane, A., Iglauer, S., 2016. Residual trapping of supercritical CO<sub>2</sub> in oil-wet sandstone. *J. Colloid Interface Sci.* 469, 63–68.
- Roshan, H., Al-Yaseri, A., Sarmadivaleh, M., Iglauer, S., 2016. On wettability of shale rocks. *J. Colloid Interface Sci.* 475, 104–111.
- Saraji, S., Goual, L., Piri, M., Plancher, H., 2013. Wettability of supercritical carbon dioxide/water/quartz systems: Simultaneous measurement of contact angle and interfacial tension at reservoir conditions. *Langmuir* 29 (23), 6856–6866.
- Sarmadivaleh, M., Al-Yaseri, A.Z., Iglauer, S., 2015. Influence of temperature and pressure on quartz–water–CO<sub>2</sub> contact angle and CO<sub>2</sub>–water interfacial tension. *J. Colloid Interface Sci.* 441, 59–64.
- Siddiqui, M.A.Q., Ali, S., Fei, H., Roshan, H., 2018. Current understanding of shale wettability: A review on contact angle measurements. *Earth-Sci. Rev.* 181, 1–11.
- Span, R., Wagner, W., 1996. A new equation of state for carbon dioxide covering the fluid region from the triple-point temperature to 1100 K at pressures up to 800 MPa. *J. Phys. Chem. Ref. Data* 25 (6), 1509–1596.
- Stalker, L., Varma, S., Van Gent, D., Haworth, J., Sharma, S., 2013. South west hub: a carbon capture and storage project. *Aust. J. Earth Sci.* 60 (1), 45–58.
- Ulrich, H.J., Stumm, W., Cosovic, B., 1988. Adsorption of aliphatic fatty acids on aquatic interfaces. Comparison between two model surfaces: the mercury electrode and  $\delta$ -Al<sub>2</sub>O<sub>3</sub> colloids. *Environ. Sci. Technol.* 22 (1), 37–41.
- van der Roest, E., Snijp, L., Fens, T., van Wijk, A., 2020. Introducing power-to-H<sub>3</sub>: Combining renewable electricity with heat, water and hydrogen production and storage in a neighbourhood. *Appl. Energy* 257, 114024.
- Yang, D., Gu, Y., Tontiwachwuthikul, P., 2007. Wettability determination of the reservoir brine- reservoir rock system with dissolution of CO<sub>2</sub> at high pressures and elevated temperatures. *Energy Fuels* 22 (1), 504–509.
- Yates, E., Bischoff, A., Beggs, M., Jackson, N., 2018. Hydrogen geo-storage in Aotearoa-New Zealand.
- Yekeen, N., et al., 2020. Wettability of rock/CO<sub>2</sub>/brine systems: A critical review of influencing parameters and recent advances. *J. Ind. Eng. Chem.* 88, 1–28.
- Yekeen, N., et al., 2021. CO<sub>2</sub>/brine interfacial tension and rock wettability at reservoir conditions: A critical review of previous studies and case study of black shale from Malaysian formation. *J. Pet. Sci. Eng.* 196, 107673.
- Yekta, A., Manceau, J.-C., Gaboreau, S., Pichavant, M., Audigane, P., 2018. Determination of hydrogen–water relative permeability and capillary pressure in sandstone: application to underground hydrogen injection in sedimentary formations. *Transp. Porous Media* 122 (2), 333–356.
- Zivar, D., Kumar, S., Foroozesh, J., 2020. Underground hydrogen storage: A comprehensive review. *Int. J. Hydrogen Energy*.
- Zivar, D., Kumar, S., Foroozesh, J., 2021. Underground hydrogen storage: A comprehensive review. *Int. J. Hydrogen Energy* 46 (45), 23436–23462.
- Zullig, J.J., Morse, J.W., 1988. Interaction of organic acids with carbonate mineral surfaces in seawater and related solutions: I. Fatty acid adsorption. *Geochim. Cosmochim. Acta* 52 (6), 1667–1678.